AD-A037 097 AEL SERVICE CORP FARMINGDALE N J F/G 20/14
ELECTROMAGNETIC RADIATION SYSTEM (EMRS) FOR SUSCEPTIBILITY TEST--ETC(U)
FEB 77 E S ISKRA DAAB07-76-C-0332
UNCLASSIFIED AELSC-TR-23-3 ECOM-76-0332-3 NL

| OF |
AD
A037097

END

DATE
FILMED
4-77

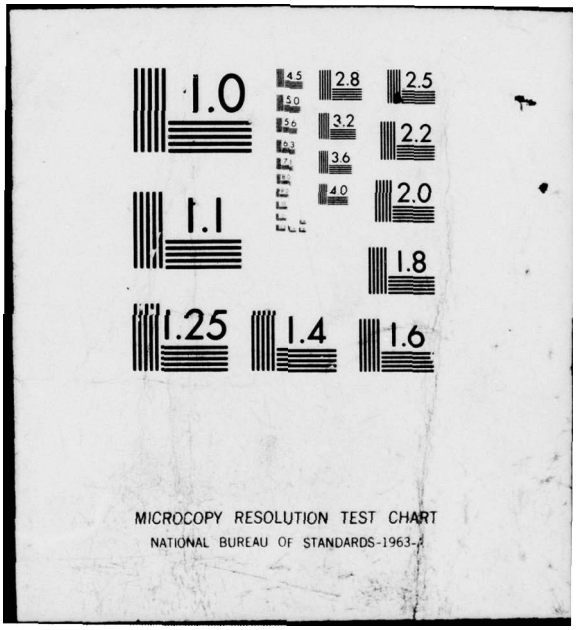
1.0
1.1
1.25
1.4
1.6
1.8
2.0
2.2
2.5
2.8
3.2
3.6
4.0
4.5
5.0
5.6
6.3
MICROCOPY RESOLUTION TEST CHART
NATIONAL BUREAU OF STANDARDS-1963-A

(12)

(8)

AD A037097

Research and Development Technical Report

ECOM- 76-0332-3

ELECTROMAGNETIC RADIATION SYSTEM (EMRS)

FOR SUSCEPTIBILITY TESTING

Edwin S. Iskra
American Electronic Laboratories, Inc.
P. O. Box 691
Farmingdale, New Jersey 07727

FEBRUARY 1977
Interim Report for Period 3 May 1976-29 October 1976

DISTRIBUTION STATEMENT

APPROVED FOR PUBLIC RELEASE;

DISTRIBUTION UNLIMITED

DDC
RECEIVED
MAR 18 1977
A

PREPARED FOR:

ECOM

US ARMY ELECTRONICS COMMAND FORT MONMOUTH, NEW JERSEY 07703

NOTICES

Disclaimers

The findings in this report are not to be construed as an official Department of the Army position, unless so designated by other authorized documents.

The citation of trade names and names of manufacturers in this report is not to be construed as official Government endorsement or approval of commercial products or services referenced herein.

Disposition

Destroy this report when it is no longer needed. Do not return it to the originator.

Research and Development Technical Report

ECOM- 76-0332-3

ELECTROMAGNETIC RADIATION SYSTEM (EMRS)

FOR SUSCEPTIBILITY TESTING

DDC
RECEIVED
MAR 18 1977
C

Edwin S. Iskra
American Electronic Laboratories, Inc.
P. O. Box 691
Farmingdale, New Jersey 07727

FEBRUARY 1977
Interim Report for Period 3 May 1976-29 October 1976

DISTRIBUTION STATEMENT

APPROVED FOR PUBLIC RELEASE;

DISTRIBUTION UNLIMITED

PREPARED FOR:

ECOM

US ARMY ELECTRONICS COMMAND FORT MONMOUTH, NEW JERSEY 07703

UNCLASSIFIED

SECURITY CLASSIFICATION OF THIS PAGE (When Data Entered)

REPORT DOCUMENTATION PAGE	READ INSTRUCTIONS BEFORE COMPLETING FORM
1. REPORT NUMBER: ECOM-76-0332-3	2. GOVT ACCESSION NO. / 3. RECIPIENT'S CATALOG NUMBER
4. TITLE (and Subtitle): ELECTROMAGNETIC RADIATION SYSTEM (EMRS) for SUSCEPTIBILITY TESTING.	5. TYPE OF REPORT & PERIOD COVERED: Interim Report. 3 May [illegible] — 29 Oct 76
	6. PERFORMING ORG. REPORT NUMBER: AELSC-TR-23-3
7. AUTHOR(s): Edwin S. Iskra	8. CONTRACT OR GRANT NUMBER(s): DAAB07-76-C-0332
9. PERFORMING ORGANIZATION NAME AND ADDRESS: American Electronic Laboratories, Inc. P.O. Box 691 Farmingdale, NJ 07727 AEL Service Corp	10. PROGRAM ELEMENT, PROJECT, TASK AREA & WORK UNIT NUMBERS: 6.27.01.A 1L7 62701 AH92 C1 071 C8
11. CONTROLLING OFFICE NAME AND ADDRESS: Communications/ADP Laboratory DRSEL-NL-RY-5 U.S. Army Electronics Command, Ft. Monmouth, NJ 07703	12. REPORT DATE: Feb[illegible] 1977 / 13. NUMBER OF PAGES: 44
14. MONITORING AGENCY NAME & ADDRESS (if different from Controlling Office)	15. SECURITY CLASS. (of this report): UNCLASSIFIED / 15a. DECLASSIFICATION/DOWNGRADING SCHEDULE

16. DISTRIBUTION STATEMENT (of this Report)

Approved for public release; distribution unlimited.

1L762701AH92

17. DISTRIBUTION STATEMENT (of the abstract entered in Block 20, if different from Report)

C1

DDC RECEIVED MAR 18 1977 C

18. SUPPLEMENTARY NOTES

19. KEY WORDS (Continue on reverse side if necessary and identify by block number)

Electromagnetic Compatibility, electromagnetic-energy.
Electromagnetic Radiation System
(EMRS)

20. ABSTRACT (Continue on reverse side if necessary and identify by block number)

The function of the Electromagnetic Radiation System (EMRS) is to generate electromagnetic energy so as to produce a constant field strength that can be automatically scanned as a function of frequency. The design objective is to cover the frequency range of 30 hertz to 40 gigahertz with field strength intensities up to 200 volts per meter. A stripline approach is described and proposed for use as the field generating device for the

OVER

DD FORM 1 JAN 73 1473 EDITION OF 1 NOV 65 IS OBSOLETE

409 710

UNCLASSIFIED

SECURITY CLASSIFICATION OF THIS PAGE (When Data Entered)

lower frequencies. The use of refocused parabolas are proposed for use at the higher frequencies.

ACCESSION for
NTIS White Section
DDC Buff Section
UNANNOUNCED
JUSTIFICATION
BY
DISTRIBUTION/AVAILABILITY C
Dist. AVAIL. and/or SP
A

TABLE OF CONTENTS

ACKNOWLEDGEMENT

Acknowledgement is made of the analytical and conceptual development of the strip transmission line technique and to the formulation of the refocused parabola concept, as applicable to EMRS requirements, by Messrs. D. Lipkin, R.Klopach and R. Hartman, of American Electronic Laboratories, Inc., Colmar, Pennsylvania.

1. INTRODUCTION

1.1 Purpose of Program.

The purpose of this program is to develop an electromagnetic radiation system (EMRS) which will produce a prescribed constant field strength while it scans a wide frequency range. The specified maximum field strength is 200 volts per meter and the specified frequency range is 30 Hz to 40 GHz. The system is intended to be used to perform electromagnetic susceptibility tests on a wide variety of test samples, to the requirements of military electromagnetic compatibility (EMC) standards.

The program consists of two phases. Phase I covers research and investigation to determine specific requirements for the EMRS and methods for meeting these requirements. The result of Phase I is a design plan of the EMRS system, resulting from the investigations performed during this phase. Phase II covers construction of an exploratory development model of the EMRS, consisting of a working model covering portions of the required frequency range. This model will be constructed after approval of the design plan by the contracting officer (or his designated representative).

1.2 Summary of Second Quarter.

During the second quarterly reporting period, the following major tasks were performed:

1. A system block diagram was developed.

2. Potential signal sources and amplifiers, which could be used in the final EMRS, were surveyed and their characteristics were tabulated.

3. The parallel plate transmission line, originally considered for low frequency field generation, was replaced by the more suitable strip transmission line.

4. Preliminary calculations were performed to determine the power required to obtain a field of 200 volts per meter with the strip line, and theoretical and experimental analysis was performed to determine the equivalence between fields generated by this line and radiated fields. The physical characteristics of the strip line and its characteristic impedance were investigated.

5. The elliptic reflector, originally considered for high frequency field generation, was replaced by the more suitable refocused parabola. Preliminary analysis of the refocused parabola was performed on a far field basis.

1.3 Summary of Third Quarter.

During the third quarterly reporting period, primary emphasis was placed on refining the design of the strip transmission line and the refocused parabola, including calculations of various design parameters. This work is

outlined below:

1. Dimensions of the strip transmission line, required to obtain a characteristic impedance of 50 ohms, were computed.

2. The effects of protrusions, on the surface of the test sample, and on the VSWR of the strip line were analyzed.

3. The maximum usable frequency of the strip line, to insure propagation of the TEM mode only, was calculated.

4. The maximum attenuation per unit length of the strip line was calculated.

5. A practical design for the strip line configuration was developed, and power required to establish the required field strength was computed.

6. For the refocused parabola, the axial displacement of the feed was computed, and it was proven experimentally that the resulting antenna had the same gain in both the near and the far field.

7. Calculations and graphs were prepared to show the gain, beam-width, field intensity, required power (for 200 volts per meter) and diameter of circle illuminated, as functions of frequency and aperture diameter.

8. An updated system block diagram was prepared, and descriptions of the various components in a functional sense are included in this report.

2. EMRS SYSTEM

2.1 Description

The EMRS block diagram is shown in Figure 1. The overall system consists of two subsystems, a low frequency system (strip transmission line) and a high frequency system (refocused parabolas). The low frequency system covers the range of frequencies from 10 kHz to 2 GHz requiring a power input over the frequency range of up to 50 watts. The high frequency system covers the range of frequencies from 2 GHz to 40 GHz. Individual bands cover 2-4 GHz, 4-8 GHz, 8-12.4 GHz, 12.4-18 GHz, 18-26.5 GHz and 26.5-40 GHz. The input power required for these bands ranges from 1 watt to over 100 watts, depending on frequency and antenna size.

To provide the required field intensity of 200 V/m over the specified frequency bands, power amplifiers are necessary. The 10 kHz to 40 GHz bandwidth is covered in 10 ranges: 10 kHz-250 MHz, 250-500 MHz, 500 MHz-1 GHz, 1-2 GHz, 2-4 GHz, 4-8 GHz, 8-12.4 GHz, 12.4-18 GHz, 18-26.5 GHz and 26.5-40 GHz. The 200 V/m field intensity over the frequency range above 2 GHz is achieved with power drive requirements as shown in Figure 9. Power amplifier requirements below 2 GHz are less than 50 watts as shown in section 3.9 of this report.

The signal sweep generators, with their respective plug-in modular units, contain built-in leveling controls. The generator output as a function of frequency is held constant by the level control. The sweep generators also contain variable gain (power out) control which control the field intensity by varying the signal generator output. The sweep generator drives a system that is broadband and relatively flat, assuring a field strength that is constant within a few dB as a function of frequency.

The EMRS system output is monitored by a power meter, which measures power output, and a frequency meter which measures the operating frequency.

2.2 Key Features

The EMRS system is capable of presetting field strengths from .001 to 200 V/m by adjusting the gain control on the sweep generators. An absolute indication of the field strength can be read off the calibrated power meter to an accuracy of better than $\pm$ 4 dB.

The EMRS system is designed to produce field intensities up to 200 V/m. To produce this intensity over the frequency band of 10 kHz to 2 GHz, a power amplifier of 50 watts is required. From 2 GHz to 40 GHz, power amplifiers from approximately 126 watts down to 1 watt, are required. If field intensities of less than 200 V/m are required (say 50 V/m), the appropriate power amplifiers can be easily integrated into the system without any other equipment changes.

The signal source for the EMRS is a sweep generator with plug-in modular units to cover the required frequency ranges shown in Figure 1. The user may select which frequency bands are needed and the corresponding plug-in units that suit his own particular needs.

The signal sweep generators have the capability to automatically and manually scan the frequency band that they cover.

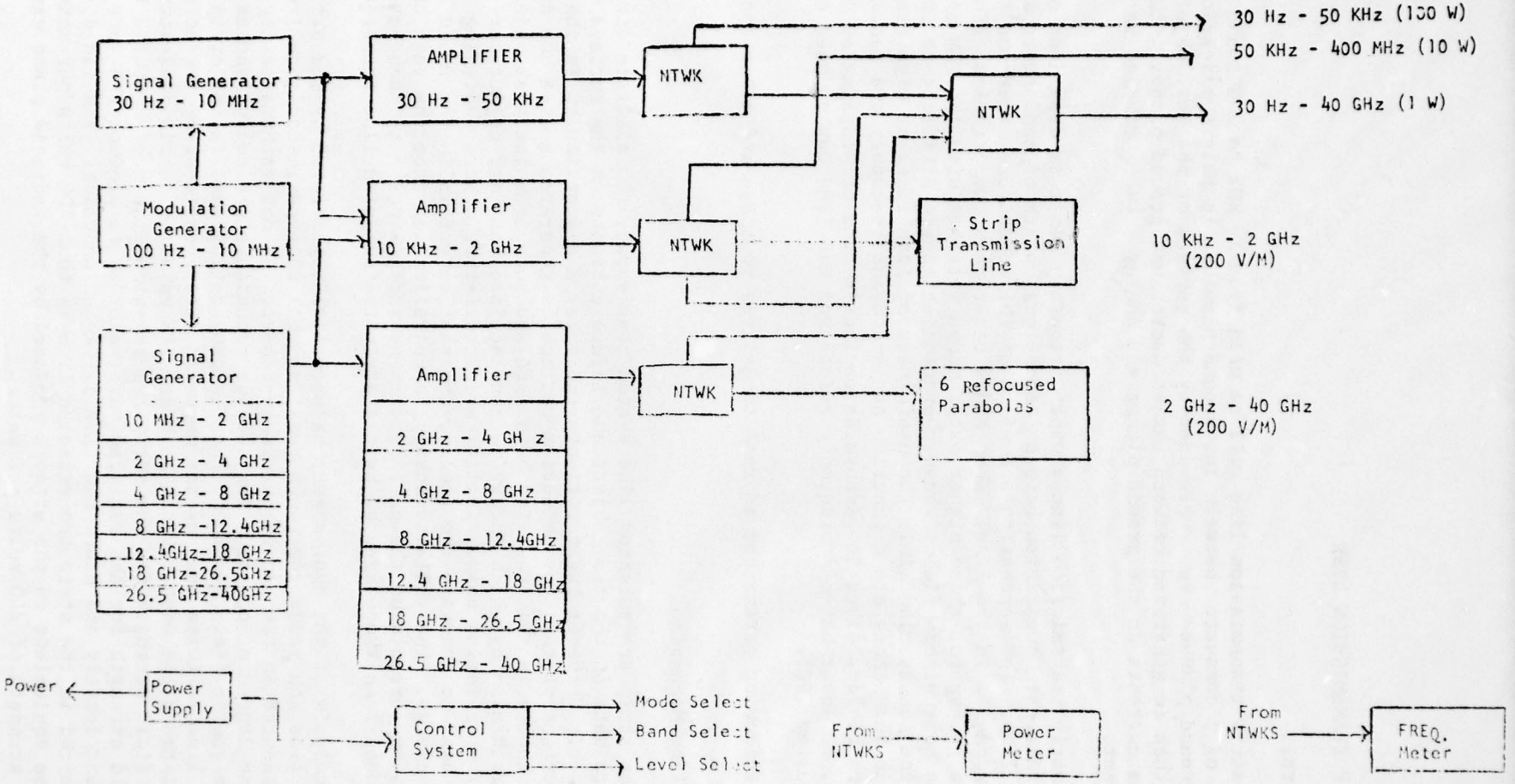

COPY AVAILABLE TO DDC DOES NOT PERMIT FULLY LEGIBLE PRODUCTION

EMRS BLOCK DIAGRAM

Figure 1

3. STRIP TRANSMISSION LINE

3.1 General.

The strip transmission line will be used from 10 kHz to 2 GHz and will consist of a conductor between two ground planes. In this application, one of the ground planes is provided by the surface of the test object. Fields will then be generated between the conductor and ground planes. These fields induce currents on the ground planes and energy is coupled into the test object.

The strip transmission line's upper frequency limit is dependent upon a number of factors: separation between conductors, width of conductors and transmission loss. The separation and width of the conductors determine the modes that propagate in the line. When modes other than the principal TEM mode begin to propagate, these higher order modes interact with the TEM mode and result in non-uniform fields whose characteristics are difficult to predict. The line losses also limit the usefulness of long lines at high frequencies since the losses are a function of length and frequency and result in non-uniform fields. Since the transmission line's mode of propagation is the TEM mode, no lower cut-off frequency exists and the line can be used down to zero frequency (DC).

The following paragraphs address themselves to these and other considerations.

3.2 Coupling Mechanism.

In the strip transmission line system considered, the electric fields generated terminate on the test object and induce currents on the surface of the test object. Whenever these currents encounter a discontinuity in the conductive surface of the test object, a voltage is generated across the discontinuity. Energy is then radiated both into and away from the test object. This is the mechanism by which energy is coupled into the test object for determining its radiation susceptibility characteristics. When radiating antennas are used to generate the fields, the test object is in the field of the radiated energy. The radiated energy, upon reflection from the test object surface, induces currents on the surface. These surface currents then behave in the same manner as those induced by the strip transmission line technique.

An analysis of the equivalency between fields generated by the strip transmission line and radiating techniques, as well as experimental confirmation, was presented in the second quarterly report. It was mathematically shown that the degree of coupling for the two techniques are equivalent as long as the magnetic field component for the propagating wave in the strip transmission line is twice that of the magnetic field component of the normally incident radiated plane wave. Since both are TEM waves in an air dielectric, the electric field strength for the strip transmission line must be twice the electric field strength for the radiated wave in order to produce the same surface current density and hence the same degree of coupling. The field strength required in the strip transmission line is thus 400 volts per meter in order to be equivalent to the effects produced by the radiated plane wave with a field strength of 200 volts per meter.

3.3 Impedance.

A formula for the characteristic impedance of a strip transmission line (which assumes a wide strip width so as to neglect the fringe fields) is given as equation (18) in the second quarterly report. A more general determination of the characteristic impedance is possible with the aid of Figure 2. The impedance curves shown are valid over the range of parameters given without any assumed restrictions as to these parameters. These curves will be used in this report for a more representative determination of the strip transmission line characteristic impedance than would be possible by using equation (18).

As a practical example, the following parameters as depicted in Figure 3 are specified as practical selections:

t = 0.125 inches = thickness of center conductor.

t/b = .05

and then, b = 2.5 inches = separation between ground planes.

For a characteristic impedance of 50 ohms, Figure 2 gives the following ratio:

w/b = 1.3

and then, w = 3.25 inches = width of center conductor

Figure 3 is an illustration of the strip transmission line configuration. The physical configuration can be realized in practical application by using dielectric standoffs to maintain the spacing.

If it is assumed that the test object has a flat conductive surface, the strip transmission line does not have to conform to irregularly shaped objects. For a non-conforming (fixed) center conductor, finite protrusions on the test object surface will produce impedance loading effects. With reasonable protrusions, the percentage cross-section area of the symmetrical line obstructed by the protrusion is small, so that the effect on the impedance of the strip transmission line is relatively small. An analysis of the impedance loading effects of protrusions in strip line is given in the Appendix. The numerical example in Section 7 of the Appendix shows that even a sizeable obstruction of one square inch would not require any impedance compensation in order to preserve a voltage standing wave ratio of only 1.2 to 1. This is true in the case of Figure 3 for reasonable obstructions under one inch in height.

3.4 Cut-Off Frequency.

An upper frequency limitation is imposed on the strip transmission line by the onset of higher order mode propagation when the plate separation is greater than one-half wavelength. The equation for determining the cut-off frequency for any higher order mode is given by:

$$f = \frac{c}{2}\sqrt{\left(\frac{m}{a}\right)^2+\left(\frac{n}{b}\right)^2} \qquad (1)^*$$

where: c = speed of light

a = width

b = height

m,n = order of the mode

*N. Marcuvitz; Waveguide Handbook; Volume 10, MIT Rad Lab Series, MCGraw Hill Book Co., 1949; pp 57, equation 3.

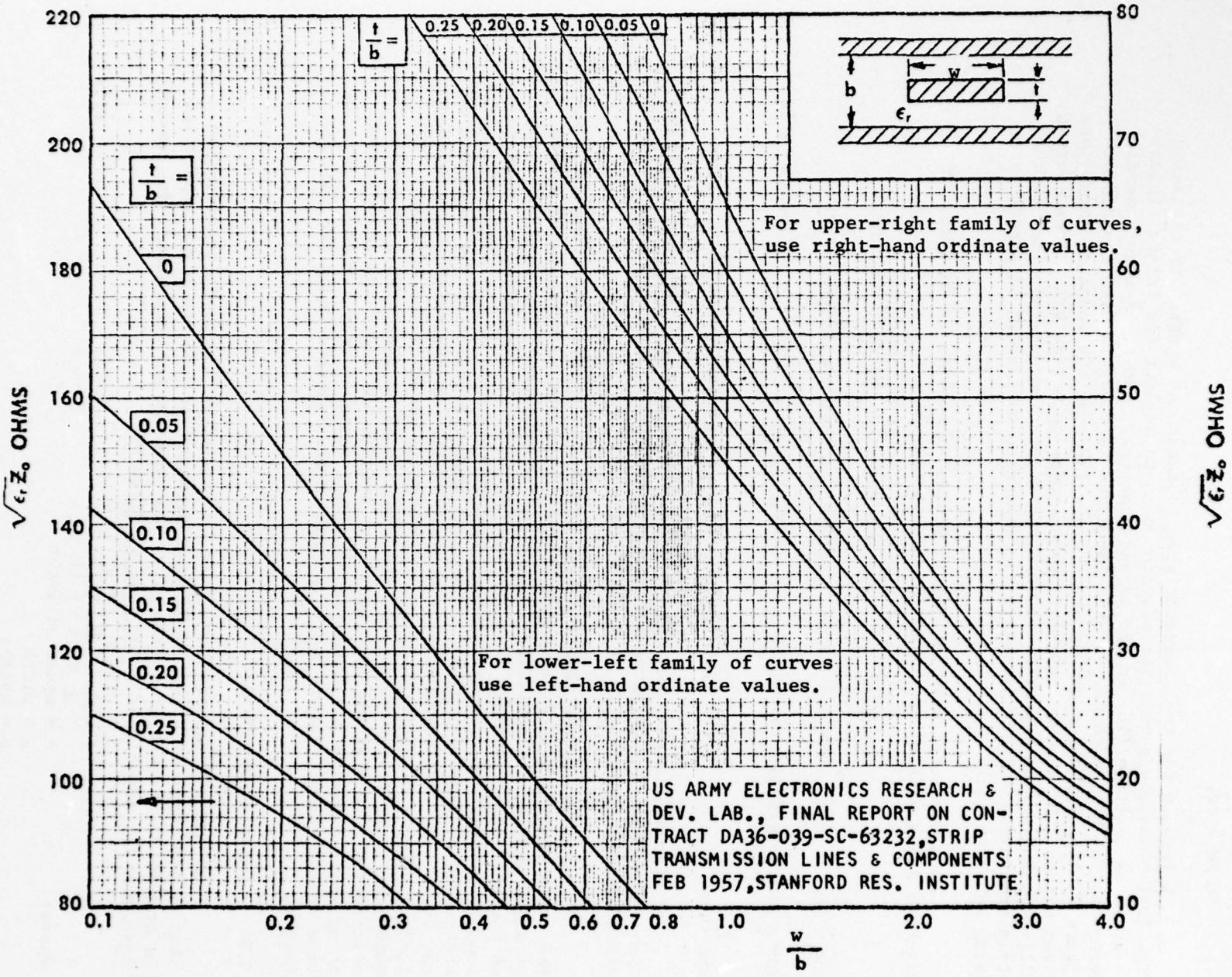

GRAPH OF $\sqrt{\epsilon_r}$ Zo VERSUS w/b FOR VARIOUS VALUES OF t/b

FIGURE 2

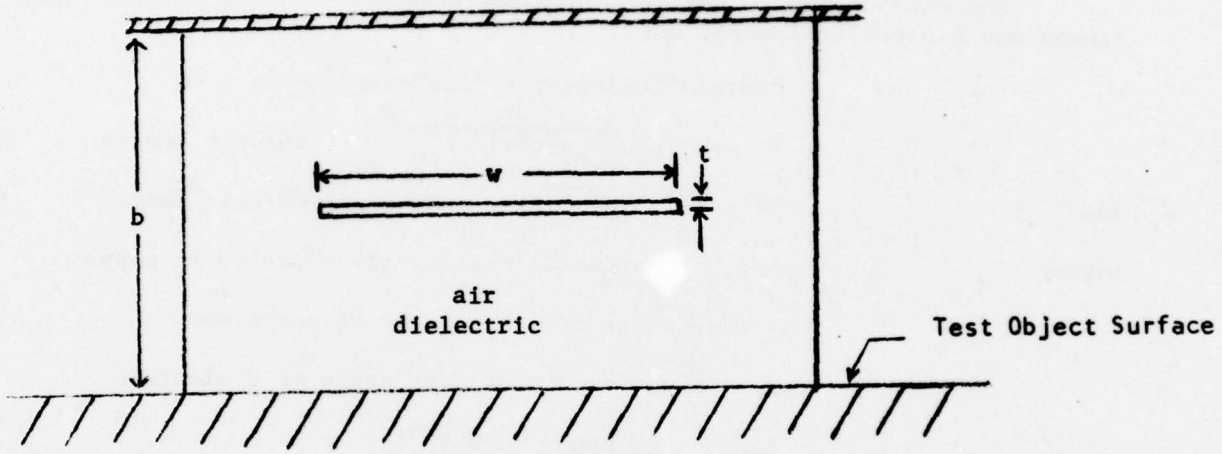

t = 0.125 inches

w = 3.25 inches

b = 2.5 inches

$\bar{z}_o$ = 50 ohms

STRIP TRANSMISSION LINE

Figure 3

The first undesired mode which will propagate is the TE_{01} mode. With m equal to zero and n equal to one, equation (1) reduces to:

$$f = \frac{c}{2b} \qquad (2)$$

For the example in Figure 3 with b equal to 2.5 inches, the upper cut-off frequency, determined by that frequency where the TE_{01} mode will propagate, is calculated to be 2.36 GHz. This indicates that the strip transmission line can be used up to 2 GHz.

3.5 Attenuation.

The attenuation in the strip transmission line is due to both conductor losses and dielectric losses, or:

$$\alpha_{total} = \alpha_{conductor} + \alpha_{dielectric} = \alpha_c + \alpha_d$$

$$\alpha_c = (y/b)\sqrt{f_{GHz}\,\epsilon_r \mu_r (\rho/\rho_{cu})} \quad \text{dB/unit length} \qquad (3)^*$$

and

$$\alpha_d = (27.3 Fp\sqrt{\epsilon_r})/\lambda_o \quad \text{dB/unit length} \qquad (4)^*$$

where

ρ/ρ_{cu} = conductor resistivity relative to copper

y = ordinate from figure 31 of reference

Fp = power factor or loss angle of dielectric

f_{GHz} = frequency in GHz

b = separation between ground planes

ϵ_r = dielectric constant

μ_r = permeability

λ_o = free-space wavelength

For the configuration being considered:

ρ/ρ_{cu} = 1.52 for aluminum conductor

y = .00052 from figure 31 (t = .125 inches, Zo = 50 ohms)

b = 2.5 inches

$\epsilon_r \approx 1.0^+$

$\mu_r \approx 1.0^+$

$Fp = .0001^+$

---

* ITT; Reference Data for Radio Engineers, Fifth Edition; pp 22-26, 27, 28.
\+ Walton, J.D.; Radome Engineering Handbook, Marcel Dekker, Inc., New York 1970; pp 193-196.

It can be seen from the equations that attenuation increases with frequency, and the greatest line loss will occur at the maximum frequency at which the stripline technique is to be used. The maximum attenuation then occurs at 2 GHz and is found to be:

$$\alpha_{dielectric} = .000462 \text{ dB/inch}$$
$$\alpha_{conductor} = .000363 \text{ dB/inch}$$

$$\alpha_{total} = .000825 \text{ dB/inch}$$

For practical purposes, the total attenuation is in the order of .01 dB per foot.

3.6 Configuration.

During the course of developing the strip transmission line technique, several configuration concepts were considered. As originally conceived, the strip transmission line would have been a flexible, though firm, structure continuously wrapped around the test object with adjacent lines appropriately spaced. This seemed extremely attractive since a 100 foot length would still have low attenuation (.01 dB per foot or 1 dB) and be able to cover large test objects in one operation. The drawback of this technique is that when the differential line length between adjacent lines becomes an odd multiple of one-half of a wavelength, the adjacent fields are 180 degrees out of phase and therefore cancel. For this reason, if the test object is to be illuminated by adjacent lines, these lines must be correlated in phase.

Another approach was to retain a flexible line structure that would be paralleled by "zip-lock" arrangements, with other identical lines to any desired width and then wrapped around the test object with only one turn of the composite line. The disadvantage of this technique is that the lines would have to be cut to appropriate lengths for each test and this would, essentially, render the lines expendable.

Rigid and flexible lines have been preliminarily investigated for mechanical implementation. Flexible lines are not mechanically desirable because the pliability of the foam or other spacing material is necessarily high to permit conformal fit to irregular surfaces and the fit is mechanically unstable on relatively smooth surfaces. A rigid line configured similar to that shown in Figure 4 is preferred. The spacing material between the top conductor surface and the center line is honeycomb or foam. Dielectric spacers are located between the striplines and the test object allowing control knobs, indicators, etc., to be closer to the stripline. The effects of these protrusions on input power and VSWR are treated in the Appendix of this report.

The stripline thus configured could be supplied in standard sizes, rectangular or square and up to 3 feet maximum dimension. In practice, several lines could be placed simultaneously over the test object to facilitate multiface coverage. If the side of the test object is less than the standard stripline sizes, the "ground plane" which is the object under test should be extended so that the stripline operates against a continuous ground plane. This may be implemented by beryllium copper spring contacts against the test object with the contacts connected to thin aluminum sheet which may be fitted to the test object or trimmed. Mechanical implementation will be determined by actual operation of prototype models so that set up time, operation cost and user convenience can be determined.

3.7 Field Variation.

In section 3.3, the width of the center conductor was established to be 3.25 inches. With the conductor width known, it is now possible to determine the field variation on the test object as a function of transverse displacement from the conductor centerline (note that the field variation longitudinally due to line losses is negligible: .03 dB for a 3 foot length). The field intensity will be maximum under the center of the conductor strip and will decrease with transverse displacement from the centerline.

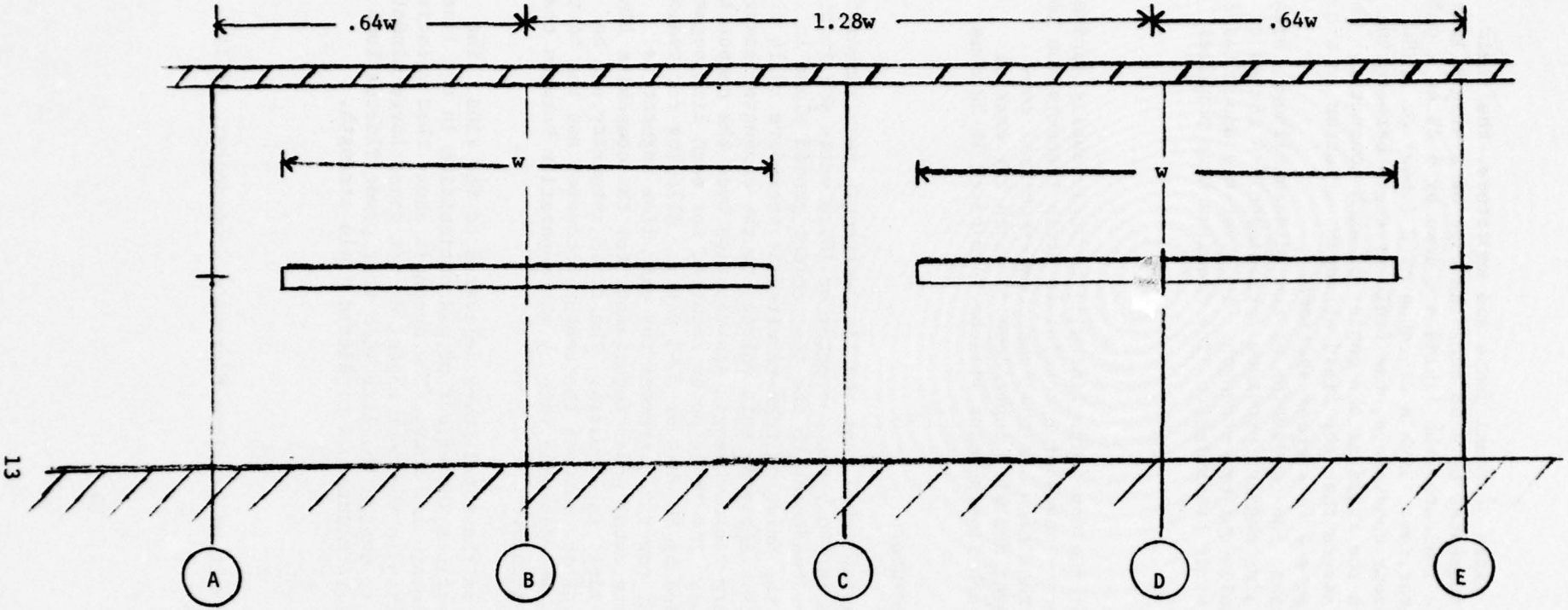

Relative field intensity generated by two adjacent in phase lines at point:

A: -6 dB

B: 0 dB (reference)

C: 0 dB

D: 0 dB

E: -6 dB

RELATIVE FIELD INTENSITY
Figure 4

When there are two adjacent lines of equal phase and amplitude, the field strength between the lines increases by 6 dB over the case of a single line. Standard data* for stripline indicates the fields are down by 6 dB at a point .64w from the conductor centerline. With a distance of 2 (.64w) or 1.28w between the centers of adjacent conductors, the field strength between the two conductors conforms with the field at the center of each conductor. This is the spacing required to assure that the field strength variation in a composite line is uniform. Figure 4 is a cross-sectional view of the strip transmission line consisting of two adjacent lines. With w equal to 3.25 inches, each line segment provides approximately 4 inches of transverse field of essentially uniform strength. To cover the specified 3 x 3 foot area, the composite strip transmission line requires nine parallel lines each 3 feet in length.

3.8 Transition Section.

Each line segment of the composite line will be individually excited by a multiport power divider by means of a coaxial to strip transmission line transition section. This transition has the same cross-sectional configuration as the line segment and will taper down to match the coaxial input. The output end of each line segment will be terminated in 50 ohms.

3.9 Input Power Requirements.

It was previously established that the field strength requirement for the strip transmission line is 400 volts per meter or 10.16 volts per inch. The distance from the center conductor to the test object ground plane in Figure 3 is 1.1875 inches; the drive voltage required is therefore 10.16 times 1.1875 inches or 12.06 volts. Applying this voltage to the conductor assures a 400 volts per meter uniform field strength distribution over the composite strip transmission line area. The input power required for each line segment is therefore $(12.06)^2$ divided by 50 ohms or 2.91 watts. Allowing for reasonable input losses, the input power requirement for each line segment is approximately 5 watts and the total power requirement for the composite line (9 individual lines in parallel) is 45 watts. The field intensity can be verified by measuring the voltage between the center conductor and the test object ground plane surface and dividing this by the separation between the conductor and test object surface.

The power required is the total power delivered to the line. The Appendix of this report describes the effect of discontinuities in the line and parallel loading to maintain low VSWR. The Appendix shows that relatively large physical discontinuities in the test object do not cause large mismatch losses, and it is possible to design the line such that power fluctuations are within the acceptable level to maintain a predicted field strength.

---

* Sanders Associates: Handbook of Triplate Microwave Components: ASTIA Document AD 110157, 1956.

4. REFOCUSED PARABOLA

4.1 Concept

The field generating system from 2 to 40 GHz will be parabolic antennas with axially refocused feeds such that the radiated energy will be focused on the test object a specified distance from the antenna.

The purpose of refocusing the feed is to simulate far field radiation patterns in the near field. Cheng* describes three techniques for determining the amount it should be axially displaced as a function of the distance at which the far field pattern is to be produced. This report concludes that the feed should be axially displaced at a distance, Δ, out from the normal focus, F, as shown in Figure 5 and as determined below:

$$\Delta = F^2/(R-F) \qquad (5)*$$

where
F = focal length
R = convergence distance
Δ = displacement distance

This relationship also shows that the amount of displacement, Δ, is not a function of frequency.

As an experimental verification, a 3 foot diameter parabola with a focal length (F) to diameter (d) ratio of 0.5 was measured at 4 GHz at a range of 80 feet ($2.19\ d^2/\lambda$), and then measured at 3 meters or 9.84 feet ($0.27\ d^2/\lambda$). From equation (5), with F equal to 18 inches and R equal to 9.84 feet or 118.08 inches, the displacement distance is 3.24 inches. The antenna was measured+ with the feed at the normal focal distance (18 inches) and at a range of 80 feet. The measured 3 dB beamwidth was 4.10 degrees. The antenna was then measured with the feed at 21.24 inches and at a range of 9.84 feet. The measured 3 dB beamwidth was 4.15 degrees. By axially refocusing the feed as predicted by equation (5), far field directivity was produced in the near field. Since the antenna efficiencies for the normally and the refocused antennas are equal, the gain in the near field and the gain in the far field are also equal.

As with the strip transmission line technique, the refocused parabola concept underwent various stages of development. Initially, as proposed in the second quarterly report, the available power was specified as 100 watts up to 12 GHz and 1 watt up to 40 GHz; the system developed was based on utilizing the available power. The resulting system consisted of eleven frequency sub-bands from 2 GHz to 40 GHz. One important conclusion drawn from this design is that high input powers are required in order to illuminate larger areas. As was pointed out in the first quarterly report, high powers at the higher frequencies are not economically practical. The system is therefore limited in the area that can be illuminated at the higher frequencies and time-scanning of larger test objects is required.

---

*D.K. Cheng; Defocus Characteristics of Microwave Reflectors; ASTIA Document, AD98167, 1955, Syracuse University, equation (35)

+The method of these pattern measurements is described in Chap. 15 "Microwave Antenna Theory & Design" by Silver.

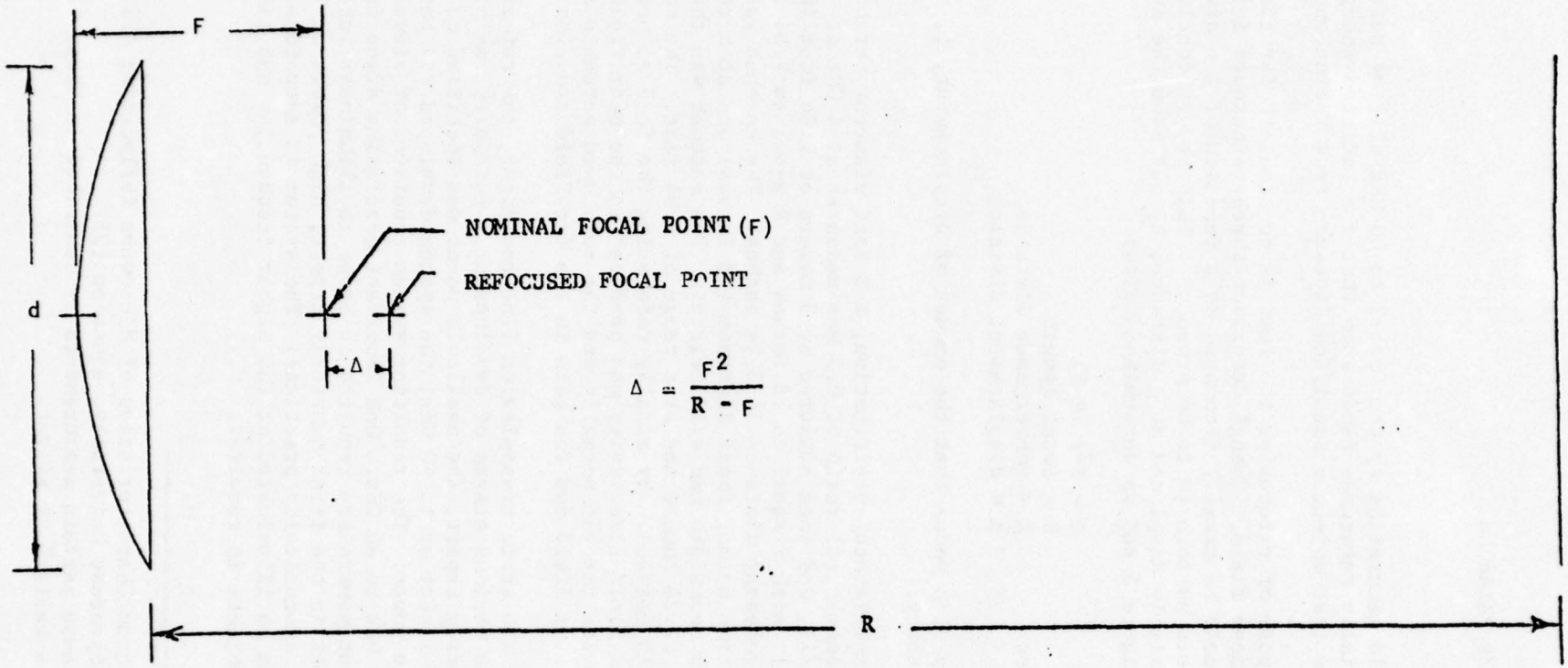

AXIALLY REFOCUSED PARABOLIC REFLECTOR

Figure 5.

Time-scanning is also desirable over the frequency bands where high power sources are available. Discussions with manufacturers have shown that the cost of a 100 watt amplifier is considerable greater than the combined cost of a 2 watt unit and scanning mechanism for each frequency band.

For reasons of economy and efficiency, the design criteria for this system is to minimize input power requirements by scanning with reflectors of reasonable size.

4.2 Configuration

A series of calculations were made to show the compromises available for the design of the 2 to 40 GHz antenna subsystem. Those parameters which are selectable are antenna size, input power, field intensity, and area illuminated. These parameters are variable within the limits of the design specification for field intensity and chamber size and within the limits of practicality of power sources.

Parabolic reflectors varying in size from 12 to 36 inches in diameter were chosen in accordance with the design specification and within the guidelines of MIL-STD-461. The antennas will be designed with refocused feeds, as discussed previously, to concentrate the antenna energy at a distance of 3 meters from the parabolic reflector. The gain of the antennas is shown in Figure 6 for antenna sizes from 12 to 36 inches in diameter. The gain was calculated from the following formula:

$$G = 0.5 \frac{4\pi A}{\lambda^2} \qquad (5)*$$

where

A = area of circular aperture
λ = wavelength

and the factor 0.5 is used for a realizable distribution on the circular aperture as described by Silver.*

The beamwidth of these antennas is shown in Figure 7 and is calculated from the following:

$$B.W. = 1.47 \frac{\lambda}{d} \qquad (6)*$$

where d is the diameter of the circular aperture and the distribution $(1-r^2)^p$ with p = 2 is used as for the gain calculations.

$r = \frac{\rho}{a}$
a = radius of the aperture
ρ = incremental radius
p = 0, 1, 2 . . .

---

* Silver, S., Microwave Antenna Theory and Design, Volume 12, MIT Rad Lab Series, McGraw Hill Book Company 1949. Section 6-8 page 192-195 and Table 6.2.

K•E 10 X 10 TO THE INCH 46 0703
7 X 10 INCHES MADE IN U.S.A.
KEUFFEL & ESSER CO.

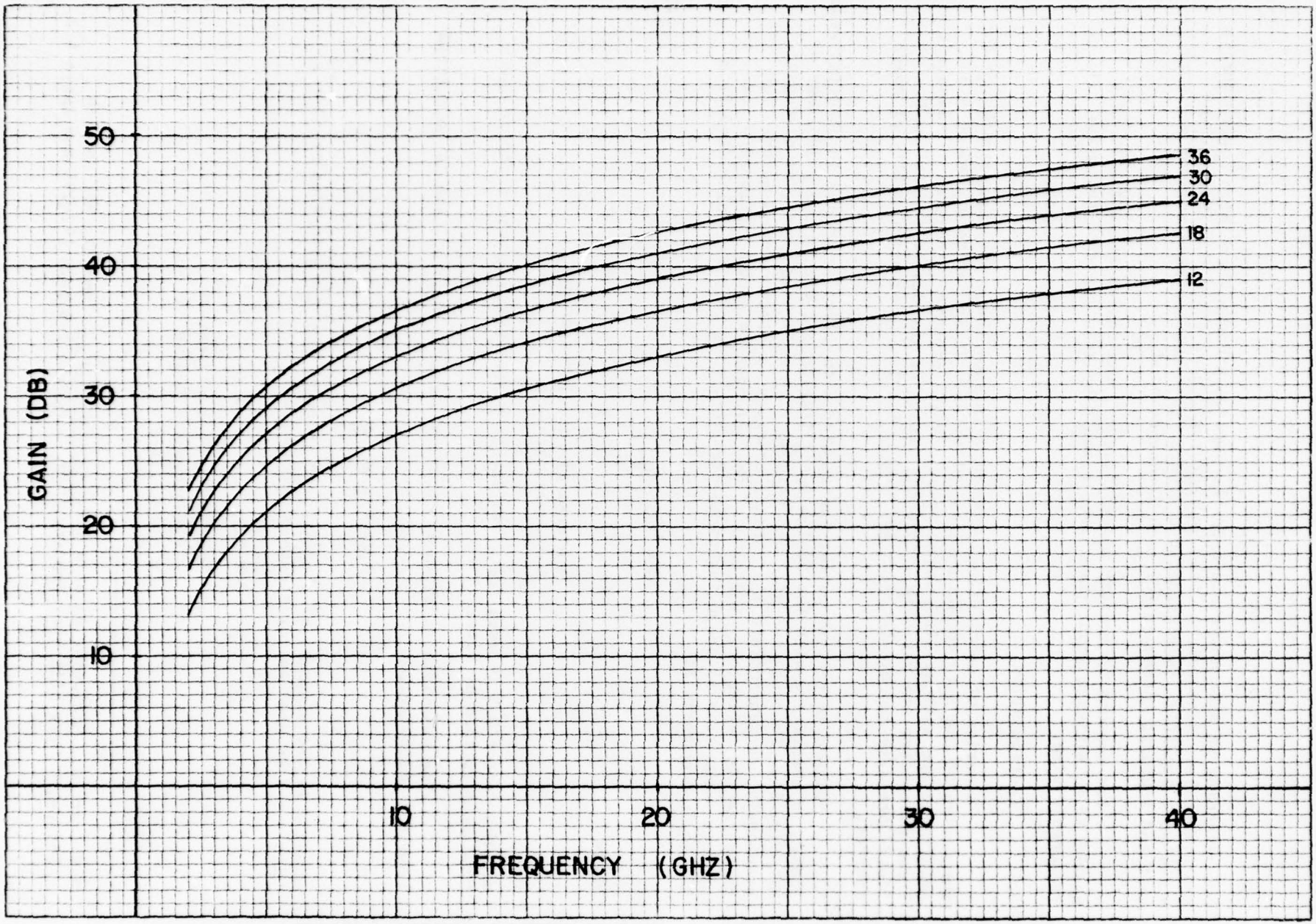

FIGURE 6. PARABOLIC REFLECTOR GAIN VS. FREQUENCY VS, ANTENNA DIAMETER

K+E 10 X 10 TO THE INCH 46 0703
KEUFFEL & ESSER CO.

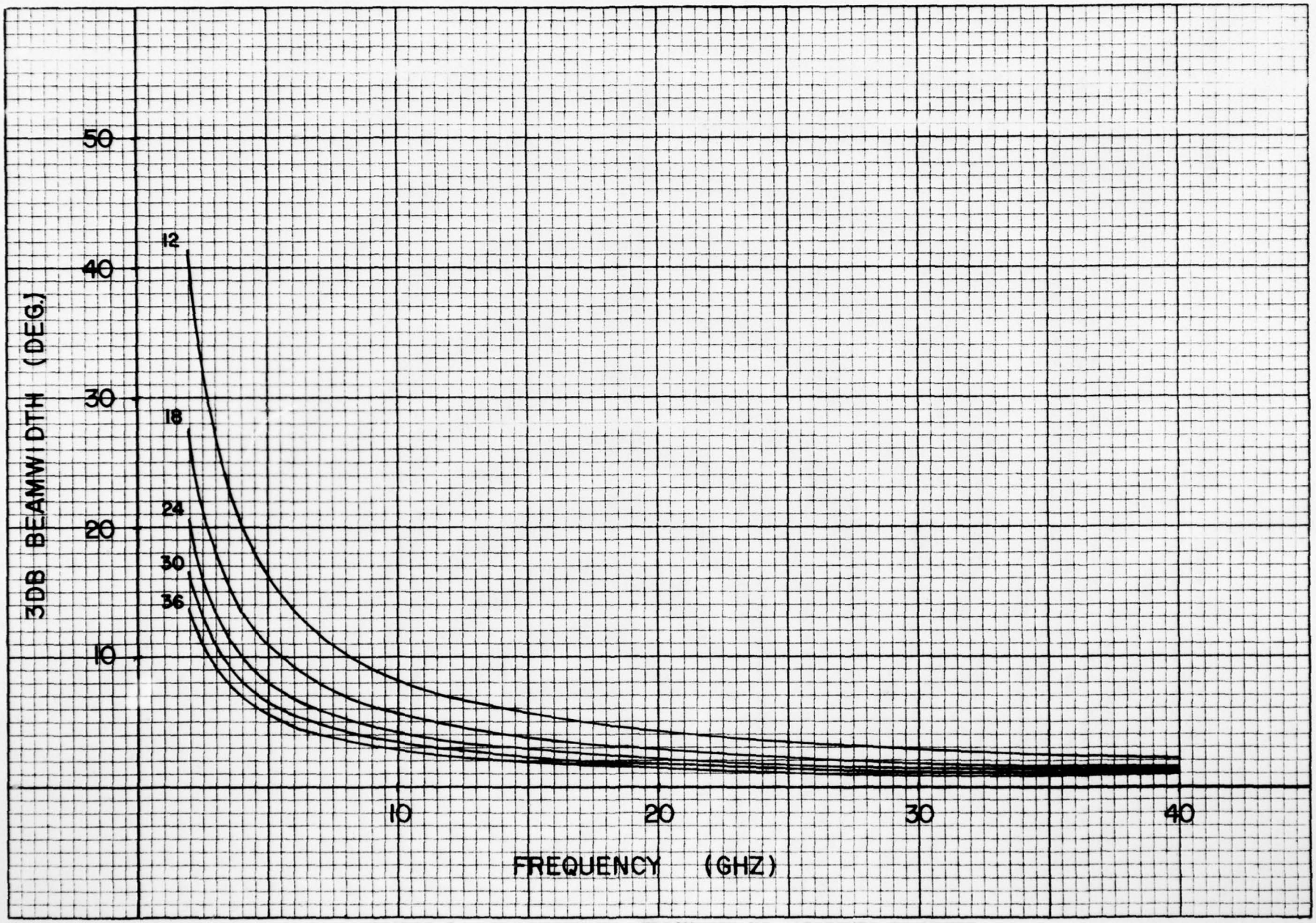

FIGURE 7. BEAMWIDTH VS. FREQUENCY VS. APERTURE DIAMETER

Choosing p = 2 is consistent with primary feed patterns readily achievable by horns or reflector backed dipole arrays.

The field intensity is calculated at the half power points of the radiation pattern. Therefore, the area included within the 6 dB points of the pattern is the calculated field intensity plus or minus 3 dB which is the excursion permitted by the design specification. The field intensity obtainable with one watt input power is shown in Figure 8 for parabolic reflectors from 12 to 36 inches in diameter.

The power required to produce a 200 volt per meter field intensity is shown in Figure 9. The power was calculated using the half power gain of the antenna. The field intensity produced between the 6 dB points of the antenna pattern is 200 V/m $\pm$ 3 dB. The power is calculated for dish sizes from 12 to 36 inches in diameter.

The parabolic antennas produce a beam with a circular cross section. The diameter of the circle illuminated by the antennas at a distance of 3 meters is shown in Figure 10 for antennas from 12 to 36 inches in diameter.

Significant conclusions pertaining to the design of the antenna subsystem are derived from the figures and summarized below:

1. Scanning is required to produce 200 V/m over a 3 foot square surface.

2. Since scanning is required, it is economically desirable to choose the larger reflectors and reduce input power requirements.

3. If 200 V/m is to be obtained using a 36 inch reflector, 126 watts of power is required at 2 GHz. (Reducing the power requirement to 10 watts would result in a dish size of approximately 9 feet which is not within the specified size guidelines.)

4. Standard parabolic reflectors between 24 and 36 inch diameter can be used in the EMRS.

KEUFFEL & ESSER CO.

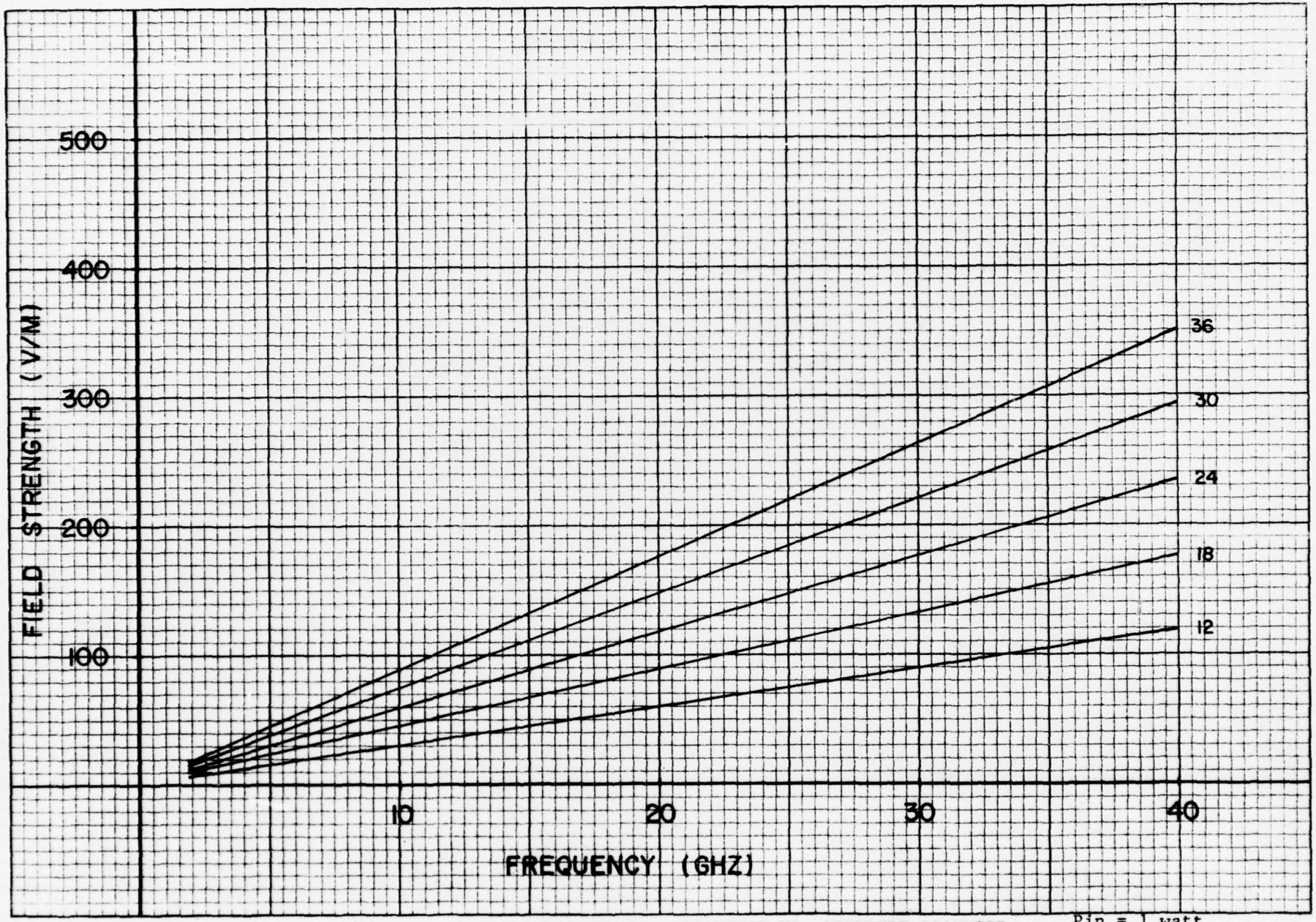

FIGURE 8. FIELD INTENSITY VS. FREQUENCY VS. APERTURE DIAMETER

Pin = 1 watt
Gain = Peak Gain - 3dB

K&E 10 X 10 TO THE INCH 46 0703
7 X 10 INCHES MADE IN U.S.A.
KEUFFEL & ESSER CO.

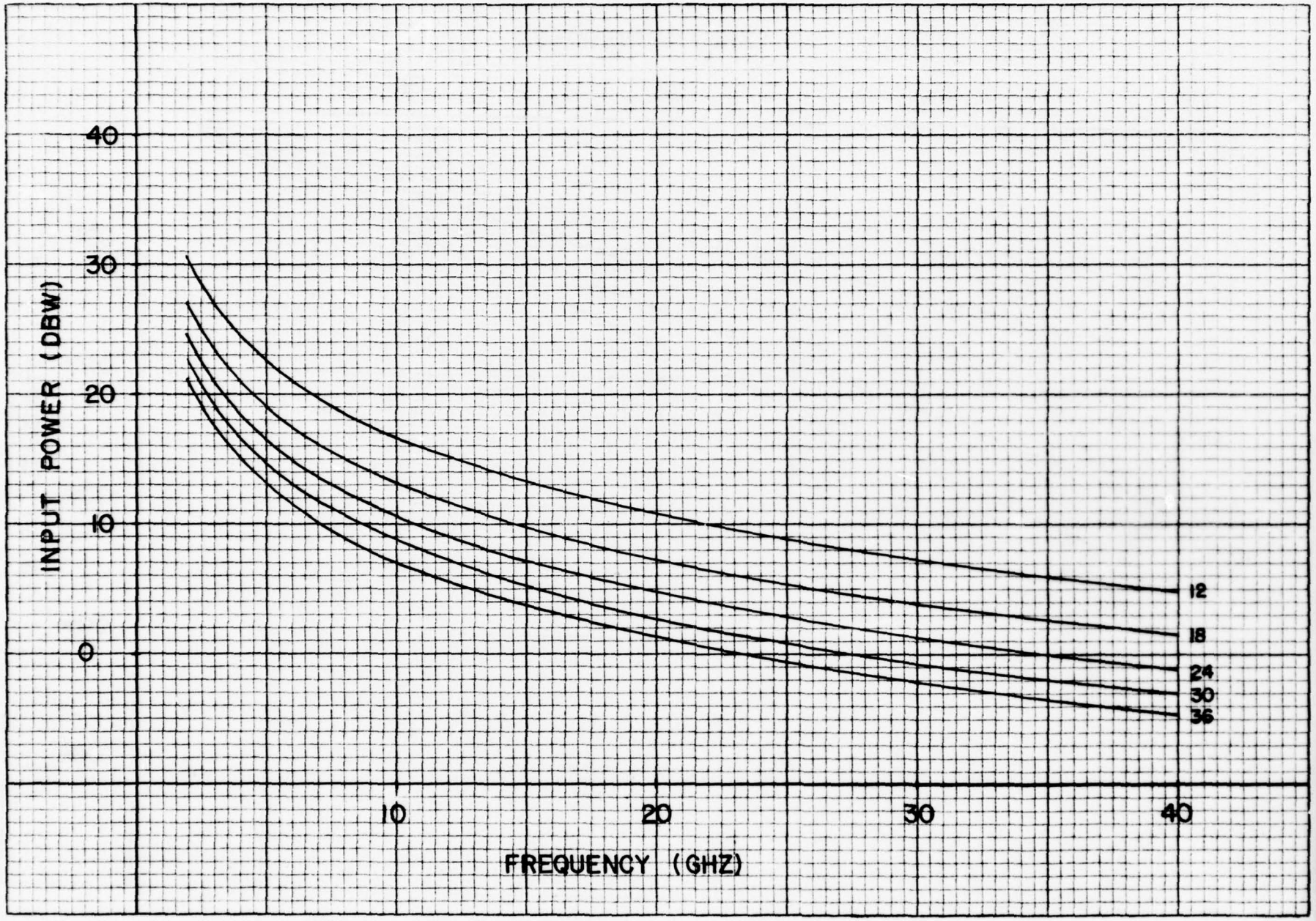

FIGURE 9. POWER REQUIRED FOR 200 V/M VS. FREQUENCY VS. APERTURE DIAMETER

KEUFFEL & ESSER CO.

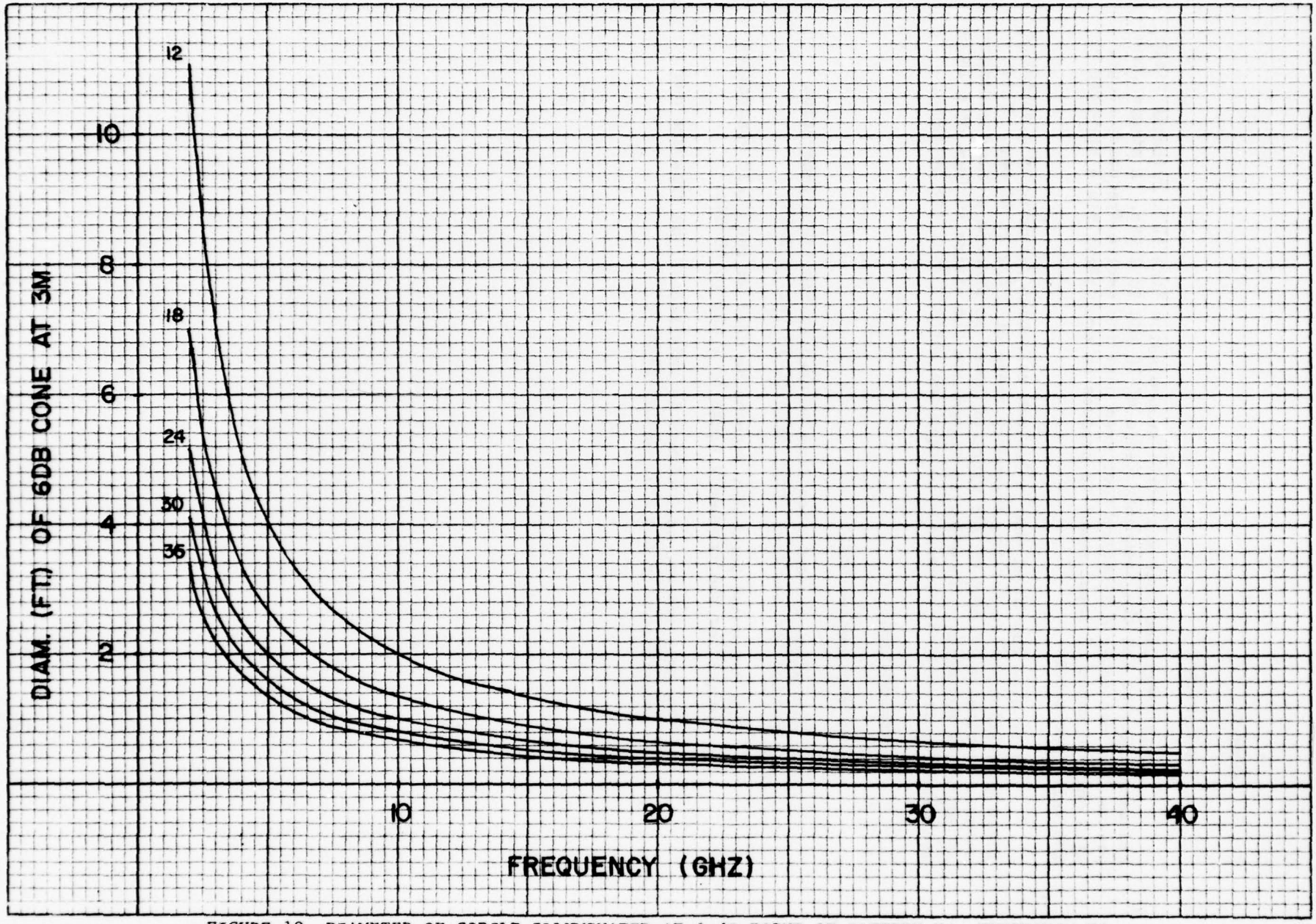

FIGURE 10. DIAMETER OF CIRCLE ILLUMINATED AT 6 dB POINT OF PATTERN VS. FREQUENCY VS. APERTURE DIAMETER

5. SUMMARY.

5.1 Conclusions.

It is concluded that the strip transmission line is a suitable field generation device for the frequency range of 10 kHz to 2 GHz. A single composite line can cover a 9-square foot area over the entire frequency range, with only 50 watts of input power to produce an equivalent field strength of 200 volts per meter.

It is also concluded that a 36-inch refocused parabola is a suitable field generation device for the frequency range of 2 GHz to 40 GHz. This antenna requires a maximum of 126 watts of power to produce a field strength of 200 volts per meter. In order to illuminate the entire surface of a large test sample, it will be necessary to scan the antenna over the surface.

5.2 Recommendations.

It is recommended that:

a. The strip transmission line be used as the field generation device for the frequency range of 10 kHz to 2 GHz.

b. The refocused parabolic antenna be used as the field generation device for the frequency range of 2 GHz to 40 GHz.

c. The EMRS system, as outlined in this report, be expanded and incorporated in the EMRS design plan.

APPENDIX

ESTIMATION OF THE DEGREE OF DUMMY-LOADING NEEDED TO CONTROL THE RETURN-VSWR TO A POWER SOURCE DRIVING AN UNPREDICTABLY OBSTRUCTED TEM LINE

Prepared by: D.M. Lipkin

NOTE: This appendix contains an analysis supporting the statement, on page 7 of the main report, regarding impedance compensation required to maintain a VSWR of 1.2:1 with a sizeable protrusion in the strip line. For a protrusion, rather than a detached obstruction, b = 0 in the diagram in this appendix.

ESTIMATION OF THE DEGREE OF DUMMY-LOADING NEEDED TO
CONTROL THE RETURN-VSWR TO A POWER SOURCE
DRIVING AN UNPREDICTABLY OBSTRUCTED TEM LINE

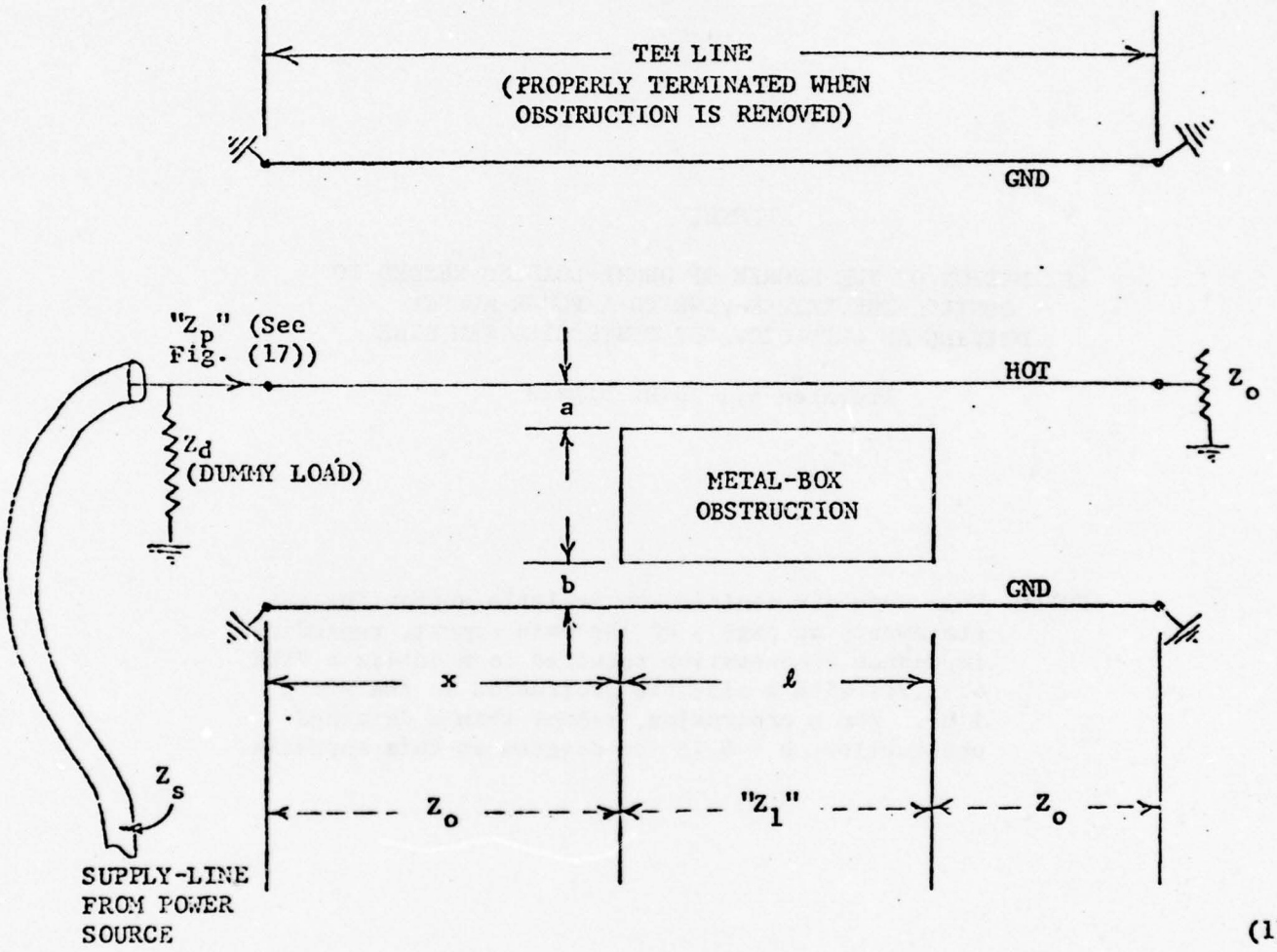

(1)

(The dimensions x, ℓ, a, and b are not predictable in advance. -- The worst case, versus both x and ℓ, is worked out, for "given", unspecified a, b, and Z_d.

1. ESTIMATION OF "Z_1" (CHARACTERISTIC IMPEDANCE OF THE OBSTRUCTED SECTION OF THE TEM LINE)

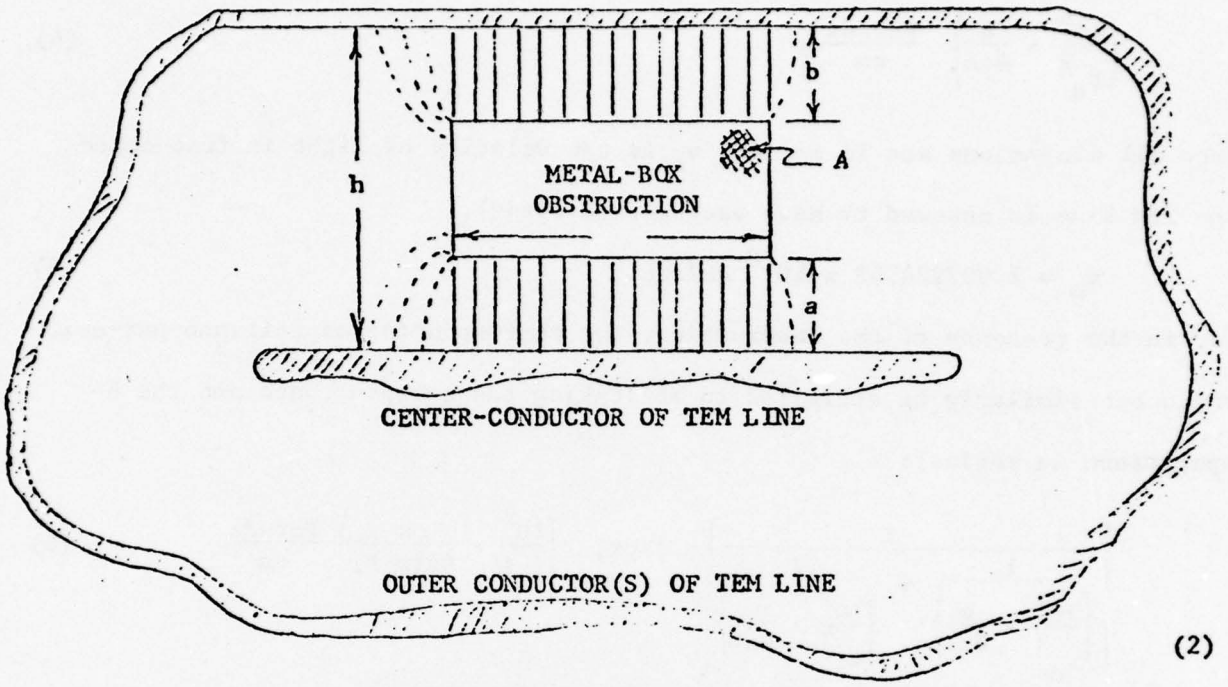

(2)

(Cross-Sectional View of Obstructed Section of the TEM Line)

For purposes of estimating the increase of the TEM lines capacitance-per-unit-length due to the presence of the obstruction, the following assumption is made:

The region of the TEM line that contains the obstruction, and the obstruction itself, have such shapes and dimensions as to enable the line's electric-field lines to be approximated as straight and of uniform density, in that region, both in the presence of, and in the absence of, the (perfectly conducting) obstruction. (3)

Subject to the assumption (3), the capacitance of the region of the TEM line of width w, per unit length along the line, in the absence of the obstruction, can be approximated as:

$$\left(\frac{10^9}{f_o^2} \cdot \frac{w}{4\pi h}\right) \quad \frac{\text{Farads}}{\text{cm}} \,, \tag{4}$$

where all dimensions are in cm, and v_o is the velocity of light in free space (the TEM line is assumed to have vacuum-dielectric):

$$v_o \equiv 2.997924562 \times 10^{10} \text{ cm/sec.} \tag{5}$$

And, in the presence of the obstruction, the corresponding capacitance-per-unit-length can similarly be estimated to be (taking the a-capacitance and the b-capacitance in series):

$$\left[\frac{1}{\frac{1}{\left(\frac{10^9}{v_o^2} \cdot \frac{w}{4\pi a}\right)} + \frac{1}{\left(\frac{10^9}{v_o^2} \cdot \frac{w}{4\pi b}\right)}}\right] \,, \text{ or, } \left(\frac{10^9}{v_o^2} \cdot \frac{w}{4\pi(a+b)}\right) \frac{\text{Farads}}{\text{cm}} \tag{6}$$

The increase in the capacitance-per-unit-length of the section of the TEM line that contains the obstruction, is therefore estimated to be: [(6)-(4)]

$$\text{"}\Delta C_1\text{"} \equiv \left[\left(\frac{10^9}{v_o^2}\right) \cdot \left(\frac{w}{4\pi}\right) \cdot \left(\frac{h-(a+b)}{(a+b)h}\right)\right] \,, \frac{\text{Farads}}{\text{cm}} \tag{7}$$

L_1 and C_1, respectively the inductance and capacitance per unit length of the unobstructed TEM line, are related to that line's characteristic impedance Z_o and velocity of propagation v_o as follows:

$$Z_o = \sqrt{\frac{L_1}{C_1}} \,, \text{ (Ohms);} \tag{8}$$

$$v_o = 1/\sqrt{L_1 C_1} \,, \text{ (cm/sec)} \tag{9}$$

in which L_1 is in Henries/cm and C_1 in Farads/cm.

The corresponding relationships for the obstructed section of the TEM line are:

$$Z_1 = \sqrt{\frac{L_1'}{C_1'}} \ , \ (\text{Ohms}); \tag{10}$$

$$v_o = 1/\sqrt{L_1' C_1'} \ , \ (\text{cm/sec}) \tag{11}$$

in which the primes denoted the altered parameters due to the obstruction, and in which it is to be noted that the same velocity-of-propagation, v_o, applies, as in the unobstructed case.

Eliminate L_1 between (8) and (9), and L_1' between (10) and (11), to get:

$$\begin{cases} C_1 = \left(\frac{1}{v_o Z_o}\right) , & (12) \\ Z_1 = \left(\frac{1}{v_o C_1'}\right) . & (13) \end{cases}$$

But,

$$C_1' = (C_1 + \Delta C_1), \tag{14}$$

where ΔC_1 is given by (7). Therefore, by eliminating C_1 between (12) and (14), and substituting the resulting expression for C_1' into (13), we obtain:

$$Z_1 = \left(\frac{Z_o}{1 + v_o Z_o \Delta C_1}\right) \tag{15}$$

By using (7) to eliminate ΔC_1 from the desired estimate, we obtain the formula: (expressing Z_1 as a fractional multiple of Z_o)

$$\left(\frac{Z_1}{Z_o}\right) \doteq \left[\frac{1}{1 + \left(\frac{10^9 Z_o}{4\pi v_o}\right) \cdot \left(\frac{[h-(a+b)]w}{(a+b)h}\right)}\right] \tag{16}$$

(which is a ratio smaller than unity, as would be expected.)

2. DETERMINATION OF THE DRIVING-POINT IMPEDANCE OF THE OBSTRUCTED TEM LINE

With reference to the Figure (1), the equivalent circuit of the entire TEM line can be represented as:

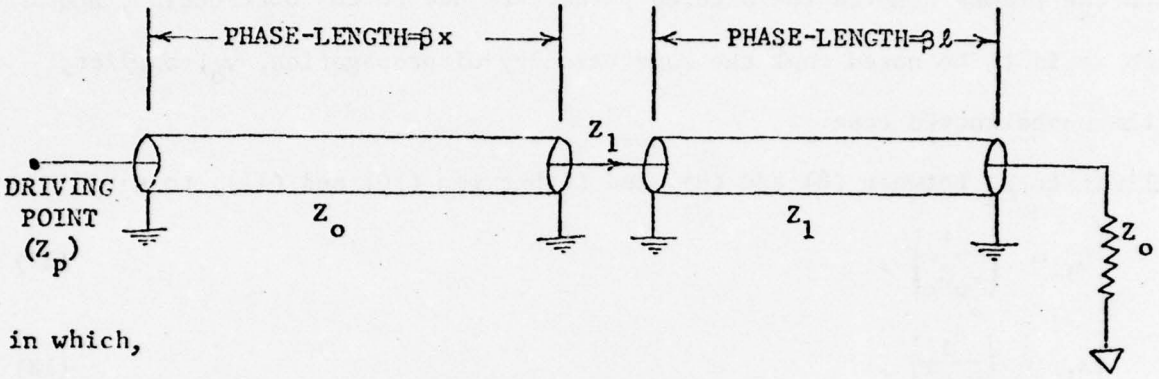

in which, (17)

$$\beta \equiv \left[\frac{2\pi}{\lambda}\right] = \left[\frac{\omega}{v_o}\right] = \left[\frac{2\pi f}{v_o}\right] . \tag{18}$$

The general formula for the impedance Z' (seen when looking into the Z_1-line, above), is:

$$Z' = \left[\frac{Z_1 (Z_o \cos(\beta\ell) + jZ_1 \sin(\beta\ell))}{(Z_1 \cos(\beta\ell) + jZ_o \sin(\beta\ell))}\right] . \tag{19}$$

Correspondingly, the desired driving-point impedance, Z_p, is:

$$Z_p = \left[\frac{Z_o(Z' \cos(\beta x) + jZ_o \sin(\beta x))}{(Z_o \cos(\beta x) + jZ' \sin(\beta x))}\right] . \tag{20}$$

By using (19) to eliminate Z' from (20), and after some rearrangement, one arrives at the following formula for Z_p:

$$\frac{Z_p}{Z_o} = \left\{ \frac{\left[\cos(\beta x)\cos(\beta \ell) - \left(\frac{Z_o}{Z_1}\right)\sin(\beta x)\sin(\beta \ell)\right]}{\left[\cos(\beta x)\cos(\beta \ell) - \left(\frac{Z_1}{Z_o}\right)\sin(\beta x)\sin(\beta \ell)\right]} \right.$$

$$\left. \frac{+\left[j\,\sin(\beta x)\cos(\beta \ell) + \left(\frac{Z_1}{Z_o}\right)\cos(\beta x)\sin(\beta \ell)\right]}{+\left[j\,\sin(\beta x)\cos(\beta \ell) + \left(\frac{Z_o}{Z_1}\right)\cos(\beta x)\sin(\beta \ell)\right]} \right\} \qquad (21)$$

(In the above formulas, Z_o and Z_1 are real impedances, and (Z_1/Z_o) may be estimated via (16). Note that $Z_p = Z_o$ if $Z_1 = Z_o$.)

For later reference, the following quantity is calculated by the use of (21):

$$\left[\frac{\left(\frac{Z_p}{Z_o} + 1\right)}{\left(\frac{Z_p}{Z_o} - 1\right)}\right] = \left\{ \frac{\left[2j\cot(\beta \ell) - \left(\frac{Z_o}{Z_1} + \frac{Z_1}{Z_o}\right)\right] e^{2j\beta x}}{\left(\frac{Z_o}{Z_1} - \frac{Z_1}{Z_o}\right)} \right\} . \qquad (22)$$

3. DETERMINATION OF THE MAGNITUDE OF THE REFLECTION-COEFFICIENT INTO THE SUPPLY-LINE

With reference to the Figures (1) and (17), the impedance that loads the supply-line Z_s is Z_p shunted by the dummy-load Z_d. The reflection-coefficient r of interest is therefore:

$$r = \left[\frac{\left(\frac{Z_p Z_d}{Z_p + Z_d} \right) - Z_s}{\left(\frac{Z_p Z_d}{Z_p + Z_d} \right) + Z_s} \right] . \tag{23}$$

We assume, however, that the supply line is properly terminated whenever the obstruction is removed from the TEM line; i.e.,

$$\{ r = 0 \text{ when } Z_p = Z_o \} . \tag{24}$$

Applying this to (23) yields:

$$Z_s = \left(\frac{Z_o Z_d}{Z_o + Z_d} \right) , \tag{25}$$

As the value to which Z_s must be designed, for any assigned choices of Z_o and Z_d. Now, (25) reduces (23) to:

$$r = \left[\frac{\left(\frac{Z_d}{Z_o} \right)}{1 + \left(1 + \frac{Z_d}{Z_o} \right) \left(\frac{\frac{Z_p}{Z_o} + 1}{\frac{Z_p}{Z_o} - 1} \right)} \right] \tag{26}$$

By substituting (22) into (26), Equation (26) is expanded to:

$$r = \left\{ \frac{\left(\frac{Z_d}{Z_o}\right)}{1 + \left[\frac{2\left(1 + \frac{Z_d}{Z_o}\right)}{\left(\frac{Z_o}{Z_1} - \frac{Z_1}{Z_o}\right)}\right] \cdot \left[j\cot(\beta\ell) - \left(\frac{\frac{Z_o}{Z_1} + \frac{Z_1}{Z_o}}{2}\right) \right] e^{2j\beta x}} \right\} \tag{27}$$

In this, we regard Z_o, Z_1, and Z_d as dissipative, positive, real impedances, and regard x and ℓ as unpredictable distances. Also, from (16), $Z_1 < Z_o$.

Patently, therefore, from the mathematical form of (27), the following upper bound can be calculated on $|r|$, for any value of x, and for unspecified fixed ℓ:

$$|r| \leq \left[\frac{\frac{Z_d}{Z_o}}{1 - \frac{2\left|1 + \left(\frac{Z_d}{Z_o}\right)\right|}{\left(\frac{Z_o}{Z_1} - \frac{Z_1}{Z_o}\right)} \sqrt{\cot^2(\beta\ell) + \left(\frac{\frac{Z_o}{Z_1} + \frac{Z_1}{Z_o}}{2}\right)^2}} \right] \tag{28}$$

(for any x)

The relationship (28) can be rewritten as follows, without absolute-value signs in the denominator:

$$|r| \leq \left[\frac{\frac{Z_d}{Z_o}}{1 + \frac{Z_d}{Z_o} \sqrt{1 + \left(\frac{4}{\left(\frac{Z_o}{Z_1} - \frac{Z_1}{Z_o}\right)^2 \sin^2(\beta\ell)}\right) - 1}} \right] \tag{29}$$

The R.H.S. of (29) reaches its largest value, a worst case, when $\sin^2(\beta \ell)$ equals unity. Therefore, in the absence of any information concerning ℓ as well as x, the following statement can nevertheless always be made:

$$(\text{for any } x,\ell) \quad |r| \leq \frac{\left(\frac{Z_d}{Z_o}\right)}{\left(1 + \frac{Z_d}{Z_o}\right)\sqrt{1 + \frac{4}{\left(\frac{Z_o}{Z_1} - \frac{Z_1}{Z_o}\right)^2}} - 1} \tag{30}$$

which can be simplified to:

$$(\text{for any } x,\ell) \quad |r| \leq \left[\frac{1}{1 + \left(\frac{2\left(1 + \frac{Z_o}{Z_d}\right)}{\left(\frac{Z_o}{Z_1}\right)^2 - 1}\right)}\right] \tag{31}$$

$$Z_o > Z_1 \text{ (see (16))}$$

which upper limit can obviously be made as close to zero as desired, by choosing the dummy-load resistance Z_d sufficiently small in value.

The VSWR in the supply-line, "v", is related to the magnitude $|r|$ of the reflection-coefficient, by:

$$v = \left(\frac{1 + |r|}{1 - |r|}\right) \left[= \left(\frac{\frac{1}{|r|} + 1}{\frac{1}{|r|} - 1}\right) = \left[1 + \frac{2}{\left(\frac{1}{|r|} - 1\right)}\right]\right] \tag{32}$$

Since this is a monotonic relationship, the upper bound (31) on $|r|$ implies the following upper bound for v:

$$v \leq \left[1 + \frac{\left[\left(\frac{Z_o}{Z_1}\right)^2 - 1\right]}{\left(1 + \frac{Z_o}{Z_d}\right)}\right] \tag{33}$$

NOTE: Independently of the value chosen for the positive resistance Z_d, the R.H.S. of (33) cannot exceed the value $(Z_o/Z_1)^2$; so, values of v greater than $(Z_o/Z_1)^2$ need never be of concern. (34)

For a specified maximum possible VSWR, "$v_{max.}$", that satisfies (34), i.e.,

$$v_{max.} < \left(\frac{Z_o}{Z_1}\right)^2, \tag{35}$$

the inequality (33) can be solved for Z_d, the dummy-load resistance, giving:

$$\left(\frac{Z_d}{Z_o}\right) \leq \left[\frac{v_{max.} - 1}{\left(\frac{Z_o}{Z_1}\right)^2 - v_{max.}}\right] \tag{36}$$

For convenience in applying the estimate (16) to (36), (16) can be rewritten as:

$$\left(\frac{Z_o}{Z_1}\right) \doteqdot \left[1 + \left(\frac{10^9\ Z_o}{4\pi\ v_o}\right) \cdot \left(\frac{(h-a-b)w}{(a+b)w}\right)\right] \tag{37}$$

From (5), we notice that: $(4\pi\ v_o/10^9) \approx$ "(120π)", and is thus just the characteristic impedance of free space:

$$\left(\frac{4\pi\ v_o}{10^9}\right) \equiv \text{"}Z_{oo}\text{"}\ (= 376.730\ \text{Ohms}). \tag{38}$$

Therefore, Equation (37) can be written still more succintly, as:

$$\left(\frac{Z_o}{Z_1}\right) \doteqdot \left[1 + \left(\frac{Z_o}{Z_{oo}}\right) \cdot \left(\frac{(h-a-b)w}{(a+b)h}\right)\right] \tag{39}$$

But, see (42)!

By inspection of the Figure (2), moreover, it is seen that the product [(h-a-b)w] which appears in (39) is just the cross-sectional area, "A", of the box-obstruction placed in the TEM line; i.e.:

$$[(h-a-b)w] \equiv A. \tag{40}$$

The product [(a+b)h] which also appears in (39) does not have as simple an interpretation, but is susceptible of representation in terms of a "mean clearance" H, as follows: Since h is the clearance (see Figure (2)) available before insertion of the obstruction, and (a+b) is the total amount of the upper and lower clearances after insertion of the obstruction, one can define a useful geometrical mean of these two clearances, by:

$$\text{"H"} \equiv \sqrt{h \cdot (a+b)}\ . \tag{41}$$

In view of (40) and (41) for notation, the formula (39) now reduces to:

$$\left(\frac{Z_o}{Z_1}\right) \div \left[1 + \left(\frac{Z_o A}{Z_{oo} H^2}\right)\right] \tag{42}$$

5. POWER-WASTE RATIO ("PWR") DUE TO THE DUMMY-LOADING

We define a PWR as follows: (see Figure (1))

"PWR" ≡ (Power Dumped Into the Dummy-Load Resistance Z_d/ Power Delivered to the TEM-Line's Termination Z_o When No Metal-Box Obstruction is present in that Line) (43)

It is readily seen, that:

$$PWR = \left(\frac{Z_o}{Z_d}\right) , \tag{44}$$

whereupon, from the inequality (36), we have the following lower limit on the PWR (connected with the use of dummy-loading to control the VSWR of the supply-line):

$$PWR \geq \left[\frac{\left(\frac{Z_o}{Z_1}\right)^2 - v_{max.}}{v_{max.} - 1}\right] , \tag{45}$$

where, again, $v_{max.}$ is a specified maximum value that the VSWR is allowed to take.

6. SUMMARY OF FORMULAS

A. The basic estimate of Z_1, the characteristic impedance of the obstructed section of the TEM line, is given via the formula (42) for (Z_o/Z_1), with (40) and (41) and (38) and their discussion providing notation, and (3) expressing an essential qualitative assumption.

B. The maximum allowable value (to allow for worst cases on the dimensions ℓ and x --- Figure (1)) for the dummy-load resistance Z_d is expressed via the inequality (36) for (Z_d/Z_o).

C. Alternatively to B., the worst VSWR that can be expected, for a given Z_d, is expressed by (33).

D. The power-waste ratio, due to dummy-loading, is as expressed by (45). -- See (43) for its definition.

E. For given TEM-line Z_o, and dummy-load Z_d, the supply-line's characteristic impedance Z_s must be as given by Equation (25).

7. NUMERICAL EXAMPLE

Choose the values:

$(a+b) = 0.5$ in. $= 1.27$ cm. (46a)

$h = 2.5$ in. $= 6.35$ cm. (46b)

$A = 1$ in.$^2 = 6.45$ cm^2 (46c)

$Z_o = 50\Omega$ (46d)

$[Z_{oo} = 376.73\Omega$ (see (38))] (46e)

$v_{max.} = 1.2{:}1$ (46f)

Then,

(41) gives "H" = 2.839 cm. (47a)

(42) gives $(Z_o/Z_1) \simeq 1.106$ $(Z_1 \simeq 45.2\Omega)$ (47b)

(36) gives $(Z_d/Z_o) \leq 8.695$ $(Z_d \leq 434.8\Omega)$ (47c)

(45) gives PWR $\geq .115$ (11.5%) (47d)

and

(25) gives $Z_s = 44.8\Omega$ (if $Z_d = 434.8\Omega$) (47e)

{Furthermore, if $Z_d = \infty$ (no dummy-loading),

(33) gives $v \leq 1.223$}, (47f)

-- so that no dummy-loading would really be required, in the context of the above example! --

DISTRIBUTION LIST

101 Defense Documentation Center
ATTN: DDC-TCA
Cameron Station (Bldg 5)
*012 Alexandria, VA 22314

104 Defense Communications Agency
Technical Library Center
Code 205
001 Washington, DC 20305

107 Director
National Security Agency
ATTN: TDL
001 Fort George G. Meade, MD 20755

108 Director, Defense Nuclear Agency
ATTN: Technical Library
001 Washington, DC 20305

110 Code R121A, Tech Library
DCA/Defense Comm Engring Ctr
1860 Wiehle Ave
001 Reston, VA 22090

200 Office of Naval Research
Code 427
001 Arlington, VA 22217

201 Commander, Naval Ship Sys Cmd
Technical Library, RM 3 S-08
National Center No. 3
001 Washington, DC 20360

202 Naval Ships Engineering Center
Code 6157D
Prince Georges Center
001 Hyattsville, MD 20782

205 Director
Naval Research Laboratory
ATTN: Code 2627
001 Washington, DC 20375

206 Commander
Naval Electronics Lab Center
ATTN: Library
001 San Diego, CA 92152

207 Commander
US Naval Ordnance Laboratory
ATTN: Technical Library
001 White Oak, Silver Spring, MD 20910

210 Commandant, Marine Corps
HQ, US Marine Corps
ATTN: Code LMC
001 Washington, DC 20380

211 HQ, US Marine Corps
ATTN: Code INTS
001 Washington, DC 20380

212 Command, Control & Comm Div
Development Center
Marine Corps Dev & Educ Cmd
001 Quantico, VA 22134

214 Commander, Naval Air Sys Cmd
Meteorological Div (AIR-540)
001 Washington, DC 20361

215 Naval Telecommunications Cmd
Tech Library, Code 422
4401 Massachusetts Ave, NW
001 Washington, DC 20390

301 Rome Air Development Center
ATTN: Documents Library (TILD)
001 Griffiss AFB, NY 13441

304 Air Force Cambridge Research Lab
L.G. Hanscom Field
ATTN: LIR
001 Bedford, MA 01730

307 HQ ESD (ZRRI)
L.G. Hanscom Field
001 Bedford, MA 01730

312 AFSPCOMMCEN/SUR
001 San Antonio, TX 78243

313 Armament Dev & Test Center
ATTN: DLOSL, Tech Library
001 Eglin Air Force Base, FL 32542

314 HQ, Air Force Systems Cmd
ATTN: DLCA
Andrews AFB
001 Washington, DC 20331

315 Director
Air University Library
ATTN: AUL/LSE-64-285
001 Maxwell AFB, AL 36112

318 HQ, AFCS
ATTN: EPECRW Mail Stop 105B
001 Richards-Gebaur AFB, MO 64030

403 HQDA(DACE-CMS)
001 WASH, DC 20310

405 OSASS-RD
001 WASH, DC 20310

406 Commander
US Army Training & Doctrine Cmd
ATTN: ATCD-SI
001 Fort Monroe, VA 23651

407 Commander
US Army Training & Doctrine CMD
ATTN: ATCD-CI
001 Fort Monroe, VA 23651

408 HQDA(DARD-ARS-P/Dr. R.B. Watson
001 WASH, DC 20310

409 CDR, DARCOM
ATTN: DRCMA-EE
5001 Eisenhower Ave
001 Alexandria, VA 22333

414 Commander
US Army Training & Doctrine Cmd
ATTN: ATCD-F
001 Fort Monroe, VA 23651

417 CDR, DARCOM
ATTN: DRCRD-01 (Mr. Speight)
5001 Eisenhower Ave
001 Alexandria, VA 22333

419 Commander
US Army Missile Command
ATTN: DRSMI-RR, Bldg 7770
001 Redstone Arsenal, AL 35809

421 CDR, US Army Missile Command
Redstone Scientific Info Ctr
ATTN: Chief, Document Section
002 Redstone Arsenal, AL 35809

422 Commander
NS Army Aeromedical Research Lab
ATTN: Library
001 Fort Rucker, AL 36362

423 Commander
US Army Armament Command
ATTN: DRSAR-RDP (Library)
001 Rock Island, IL 61201

427 CDR, US Army Combined Arms
Combat Developments Activity
ATTN: ATCAIC-IE
002 Fort Leavenworth, KS 66027

429 Commander
US Army Logistics Center
ATTN: ATCL-MA
001 Fort Lee, VA 23801

430 Commandant
US Army Ordnance School
ATTN: ATSOR-CTD
001 Aberdeen Proving Ground, MD 21005

431 Commander
US Army Intelligence School
ATTN: ATSIT-CTD
001 Fort Huachuca, AZ 85613

432 Commandant
US Army Field Artillery School
ATTN: ATSFA-CTD
001 Fort Sill, OK 73503

433 CDR, US Army Aviation Sys Cmd
ATTN: DRSAV-G
PO Box 209
001 St. Louis, MO 63166

442 Commander
Harry Diamond Laboratories
ATTN: Library
2800 Powder Mill Rd.
001 Adelphia, MD 20783

448 Commander
Picatinny Arsenal
ATTN: SARPA-ND-A-4 (Bldg 95)
001 Dover, NJ 07801

449 Commander
Picatinny Arsenal
ATTN: SARPA-TS-S #59
002 Dover, NJ 07801

450 Commander
Frankford Arsenal
ATTN: Library, K2400, BL.51-2
001 Philadelphia, PA 19137

452 Commander
Frankford Arsenal
ATTN: SARFA Z1000 (Mr. Kerensky)
001 Philadelphia, PA 19137

455 Commander
White Sands Missile Range
ATTN: STEWS-ID-S HQ
001 White Sands Missile Range, NM 88002

458 Dir/Dev & Engr
Defense Systems Div
ATTN: SAREA-DE-DDR, H. Tannenbaum
002 Edgewood Arsenal, APG, MD 21010

465 Commander
Aberdeen Proving Ground
ATTN: STEAP-TL (Bldg 305)
002 Aberdeen Proving Ground, MD 21005

474 Director
US Army Human Eng Labs
001 Aberdeen Proving Gd, MD 21005

475 Commander
HQ, Fort Huachuca
ATTN: Technical Ref Div
002 Fort Huachuca, AZ 85613

476 Commander
US Army Electronic Proving Gd
ATTN: STEEP-MT
002 Fort Huachuca, AZ 85613

480 Commander
USASA Test & Evaluation Ctr
001 Fort Huachuca, AZ 85613

482 Commander
US Army Communications Command
ATTN: ACC-FD-M
001 Fort Huachuca, AZ 85613

483 Commander
US Army Research Office
ATTN: DRXRO-IP
P.O. Box 12211
001 Research Triangle Park, NC 27709

484 Commander
US Army Research Office
ATTN: Dr. Robert J. Lontz, DRXRO-PH
P.O.Box 12211
001 Research Triangle Park, NC 27709

488 US Army Security Agency
ATTN: IARD
Arlington Hall Station
001 Arlington, VA 22212

489 Commander
US Army Tank-Automotive Command
ATTN: DRSTA-RW-L
001 Warren, MI 48090

490 Commander
Edgewood Arsenal
ATTN: SAREA-TS-L
001 Aberdeen Proving Ground, MD 21010

500 Commander
US Army Yuma Proving Ground
ATTN: STEYP-MTD (Tech Library)
002 Yuma, AZ 85364

505 CDR, US Army Security Agency
ATTN: IARD-T
Arlington Hall Station
001 Arlington, VA 22212

511 Commander
US Army Nuclear Agency
001 Fort Bliss, TX 79916

515 Director
Joint Comm Office (TRI-TAC)
ATTN: TT-AD(Tech Docu Ctr)
001 Fort Monmouth, NJ 07703

517 Commander
US Army Missile Command
ATTN: DRSMI-RE (Mr. Pittman)
001 Redstone Arsenal, AL 35809

519 Commander
US Army Systems Analysis Agency
ATTN: DRXSY-T (Mr. A. Reid)
001 Aberdeen Proving Ground, MD 21005

525 Project Manager, REMBASS
ATTN: DRCPM-RBS
001 Fort Monmouth, NJ 07703

526 Project Manager, NAVCON
ATTN: DRCPM-NC-TM (T. Daniels)
Bldg 2539
001 Fort Monmouth, NJ 07703

596 Commandant
US Army Signal School
ATTN: ATSN-CTD-MS
002 Fort Gordon, GA 30905

598 Commander
US Army Satellite Comm Agency
ATTN: DRCPM-SC-3
001 Fort Monmouth, NJ 07703

599 TRI-TAC Office
ATTN: CSS (Dr. Pritchard)
001 Fort Monmouth, NJ 07703

607 Commander
US Army Tank-Automotive Cmd
ATTN: DRSTA-RHP, Dr. J. Parks
001 Warren, MI 48090

613 Atmospheric Sciences Lab, ECOM
ATTN: DRSEL-BL-SY-L
001 White Sands Missile Range, NM 88002

617 Chief
Intel Material Dev & Support Ofc
Electronic Warfare Lab, ECOM
001 Fort Meade, MD 20755

6S0 Commander
US Army Electronics Command
000 Fort Monmouth, NJ 07703

1 DRSEL-PL-ST
1 DRSEL-VL-D
1 DRSEL-PP-I-PI
1 DRSEL-WL-D
1 DRSEL-TL-D
3 DRSEL-CT-D
1 DRSEL-BL-D
3 DRSEL-NL-RY-5
1 DRSEL-NL-D-5 (Ofc of Record)
1 DRSEL-SI-CM
1 DRSEL-MA-MP
2 DRSEL-MS-TI
1 DRSEL-GG-TD
1 DRCPM-AA
1 DRSEL-CG (Mr. Doxey)
2 DRSEL-PA
1 DRCPM-TDS-SE
1 USMC-LNO
1 DRSEL-GS-H
1 DRSEL-RD
1 TRADOC-LNO

610 Director, Night Vision Laboratory
US Army Electronics Command
ATTN: DRSEL-NV-D
001 Fort Belvoir, VA 22060

701 MIT-Lincoln Laboratory
ATTN: Library, Rm A-082
P.O. Box 73
001 Lexington, MA 02173

703 NASA Scientific & Tech Info
Facility
ATTN: Acquisitions BR (S-AK/DL)
002 College Park, MD 20740